analyzers. *Phys. Rev. Lett.* **49,** 1804–1807 (1982).
10. Ou, Z. Y. & Mandel, L. Violation of Bell's inequality and classical probability in a two-photon correlation experiment. *Phys. Rev. Lett.* **61,** 50–53 (1988).
11. Shih, Y. H. & Alley, C. O. New type of Einstein-Podolsky-Rosen-Bohm experiment using pairs of light quanta produced by optical parametric down conversion. *Phys. Rev. Lett.* **61,** 2921–2924 (1988).
12. Tapster, P. R., Rarity, J. G. & Owens, P. C. M. Violation of Bell's inequality over 4 km of optical fiber. *Phys. Rev. Lett.* **73,** 1923–1926 (1994).
13. Kwiat, P. G., Mattle, K., Weinfurter, H. & Zeilinger, A. New high-intensity source of polarization-entangled photon pairs. *Phys. Rev. Lett.* **75,** 4337–4341 (1995).
14. Tittel, W., Brendel, J., Zbinden, H. & Gisin, N. Violation of Bell inequalities by photons more than 10 km apart. *Phys. Rev. Lett.* **81,** 3563–3566 (1998).
15. Weihs, G. *et al.* Violation of Bell's inequality under strict Einstein locality conditions. *Phys. Rev. Lett.* **81,** 5039–5043 (1998).
16. Aspect, A. Bell's inequality test: more ideal than ever. *Nature* **398,** 189–190 (1999).
17. Gisin, N. & Zbinden, H. Bell inequality and the locality loophole: active versus passive switches. *Phys. Lett. A* **264,** 103–107 (1999).
18. Lo, T. K. & Shimony, A. Proposed molecular test of local hidden-variable theories. *Phys. Rev. A* **23,** 3003–3012 (1981).
19. Kwiat, P. G., Eberhard, P. H., Steinberg, A. M. & Chiao, R. Y. Proposal for a loophole-free Bell inequality experiment. *Phys. Rev. A* **49,** 3209–3220 (1994).
20. Huelga, S. F., Ferrero, M. & Santos, E. Loophole-free test of the Bell inequality. *Phys. Rev. A* **51,** 5008–5011 (1995).
21. Fry, E. S., Walther, T. & Li, S. Proposal for a loophole free test of the Bell inequalities. *Phys. Rev. A* **52,** 4381–4395 (1995).
22. Freyberger, M., Aravind, P. K., Horne, M. A. & Shimony, A. Proposed test of Bell's inequality without a detection loophole by using entangled Rydberg atoms. *Phys. Rev. A* **53,** 1232–1244 (1996).
23. Brif, C. & Mann, A. Testing Bell's inequality with two-level atoms via population spectroscopy. *Europhys. Lett.* **49,** 1–7 (2000).
24. Beige, A., Munro, W. J. & Knight, P. L. A Bell's inequality test with entangled atoms. *Phys. Rev. A* **62,** 052102-1–052102-9 (2000).
25. Lamehi-Rachti, M. & Mittig, W. Quantum mechanics and hidden variables: a test of Bell's inequality by the measurement of the spin correlation in low-energy proton–proton scattering. *Phys. Rev. D* **14,** 2543–2555 (1976).
26. Hagley, E. *et al.* Generation of Einstein-Podolsky-Rosen pairs of atoms. *Phys. Rev. Lett.* **79,** 1–5 (1997).
27. Sackett, C. A. *et al.* Experimental entanglement of four particles. *Nature* **404,** 256–259 (2000).
28. Feynman, R. P., Vernon, F. L. & Hellwarth, R. W. Geometrical representation of the Schrödinger equation for solving maser problems. *J. Appl. Phys.* **28,** 49–52 (1957).
29. Richter, T. Cooperative resonance fluorescence from two atoms experiencing different driving fields. *Optica Acta* **30,** 1769–1780 (1983).
30. Eichmann, U. *et al.* Young's interference experiment with light scattered from two atoms. *Phys. Rev. Lett.* **70,** 2359–2362 (1993).

Acknowledgements

We thank A. Ben-Kish, J. Bollinger, J. Britton, N. Gisin, P. Knight, P. Kwiat and I. Percival for useful discussions and comments on the manuscript. This work was supported by the US National Security Agency (NSA) and the Advanced Research and Development Activity (ARDA), the US Office of Naval Research, and the US Army Research Office. This paper is a contribution of the National Institute of Standards and Technology and is not subject to US copyright.

Correspondence and requests for materials should be addressed to D.J.W. (e-mail: david.wineland@boulder.nist.gov).

Autonomic healing of polymer composites

S. R. White*, N. R. Sottos†, P. H. Geubelle*, J. S. Moore‡, M. R. Kessler†, S. R. Sriram‡, E. N. Brown† & S. Viswanathan*

** Department of Aeronautical and Astronautical Engineering, † Department of Theoretical and Applied Mechanics, ‡ Department of Chemistry, University of Illinois at Urbana-Champaign, Urbana, Illinois 61801, USA*

Structural polymers are susceptible to damage in the form of cracks, which form deep within the structure where detection is difficult and repair is almost impossible. Cracking leads to mechanical degradation[1–3] of fibre-reinforced polymer composites; in microelectronic polymeric components it can also lead to electrical failure[4]. Microcracking induced by thermal and mechanical fatigue is also a long-standing problem in polymer adhesives[5]. Regardless of the application, once cracks have formed within polymeric materials, the integrity of the structure is significantly compromised. Experiments exploring the concept of self-repair have been previously reported[6–8], but the only successful crack-healing methods that have been reported so far require some form of manual intervention[10–18]. Here we report a structural polymeric material with the ability to autonomically heal cracks. The material incorporates a microencapsulated healing agent that is released upon crack intrusion. Polymerization of the healing agent is then triggered by contact with an embedded catalyst, bonding the crack faces. Our fracture experiments yield as much as 75% recovery in toughness, and we expect that our approach will be applicable to other brittle materials systems (including ceramics and glasses).

Figure 1 illustrates our autonomic healing concept. Healing is accomplished by incorporating a microencapsulated healing agent and a catalytic chemical trigger within an epoxy matrix. An approaching crack ruptures embedded microcapsules, releasing healing agent into the crack plane through capillary action. Polymerization of the healing agent is triggered by contact with the embedded catalyst, bonding the crack faces. The damage-induced triggering mechanism provides site-specific autonomic control of repair. An additional unique feature of our healing concept is the use of living (that is, having unterminated chain-ends) polymerization catalysts, thus enabling multiple healing events. Engineering this self-healing composite involves the challenge of combining polymer science, experimental and analytical mechanics, and composites processing principles.

We began by analysing the effects of microcapsule geometry and properties on the mechanical triggering process. For example, capsule walls that are too thick will not rupture when the crack approaches, whereas capsules with very thin walls will break during processing. Other relevant design parameters are the toughness and the relative stiffness of the microcapsules, and the strength of the interface between the microcapsule and the matrix. Micromechanical modelling with the aid of the Eshelby–Mura equivalent inclusion method[19] has been used to study various aspects of the complex three-dimensional interaction between a crack and a microcapsule. An illustrative result from these studies is presented in Fig. 2a, which shows the effect of the relative stiffness of the microcapsule on the propagation path of an approaching crack. The crack, the sphere and the surrounding matrix are subjected to a far-field tensile loading, σ_∞, perpendicular to the crack plane.

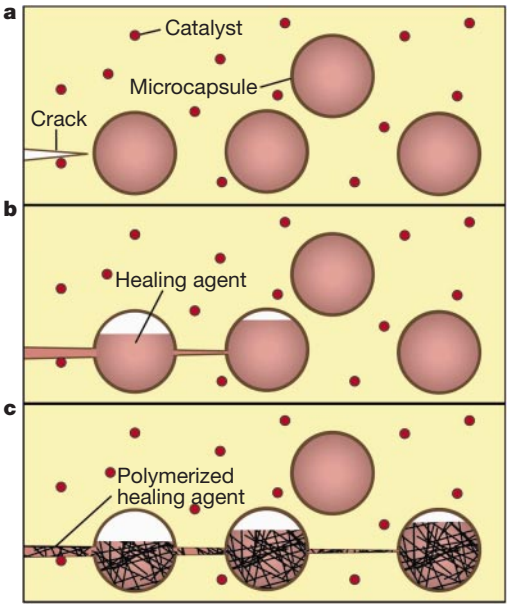

Figure 1 The autonomic healing concept. A microencapsulated healing agent is embedded in a structural composite matrix containing a catalyst capable of polymerizing the healing agent. **a**, Cracks form in the matrix wherever damage occurs; **b**, the crack ruptures the microcapsules, releasing the healing agent into the crack plane through capillary action; **c**, the healing agent contacts the catalyst, triggering polymerization that bonds the crack faces closed.

As apparent from the σ_{22} stress distribution in the equatorial plane of the sphere in Fig. 2a, the stiffness of the sphere relative to the matrix strongly affects the stress state in the proximity of the crack tip and around the sphere itself. In the case of a stiffer inclusion, the stress field in the immediate vicinity of the crack tip shows an asymmetry that indicates an undesirable tendency of the crack to be deflected away from the inclusion. The situation is reversed in the case of a more compliant spherical inclusion, and the crack is attracted toward the microcapsule, a necessary condition for its rupture and the triggering of the healing process.

Observations by optical and scanning electron microscopy confirmed the healing concept in Fig. 1 and substantiated the main findings from analytical studies in Fig. 2a. The time sequence of optical images in Fig. 2b shows the rupture of an embedded microcapsule filled with a red dye and the subsequent release of the healing agent into the crack plane. The scanning electron

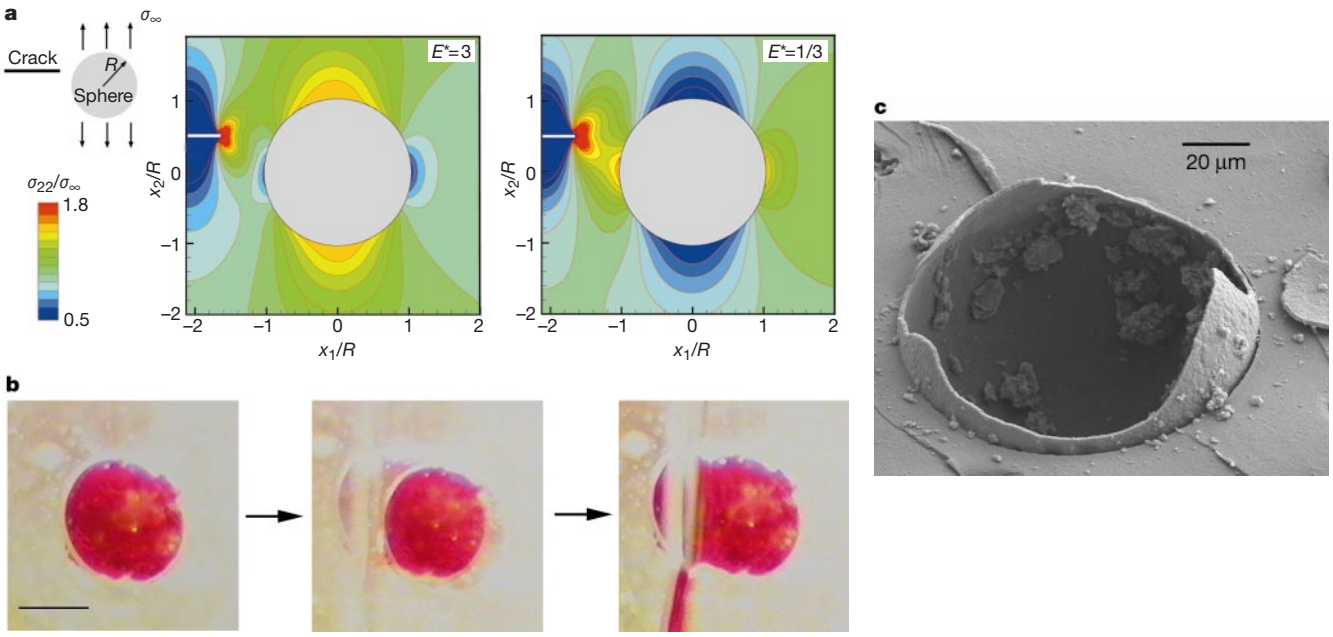

Figure 2 Rupture and release of the microencapsulated healing agent. **a**, Stress state in the vicinity of a planar crack as it approaches a spherical inclusion embedded in a linearly elastic matrix and subjected to a remote tensile loading perpendicular to the fracture plane. The left and right figures correspond to an inclusion three times stiffer ($E^* = E_{sphere}/E_{matrix} = 3$) and three times more compliant ($E^* = 1/3$) than the surrounding matrix, respectively. The Poisson's ratios of the sphere and matrix are equal (0.30). **b**, A time sequence of video images shows the rupture of a microcapsule and the release of the healing agent. A red dye was added for visualization. The elapsed time from the left to right image is 1/15 s. Scale bar, 0.25 mm. **c**, A scanning electron microscope image shows the fracture plane of a self-healing material with a ruptured urea-formaldehyde microcapsule in a thermosetting matrix.

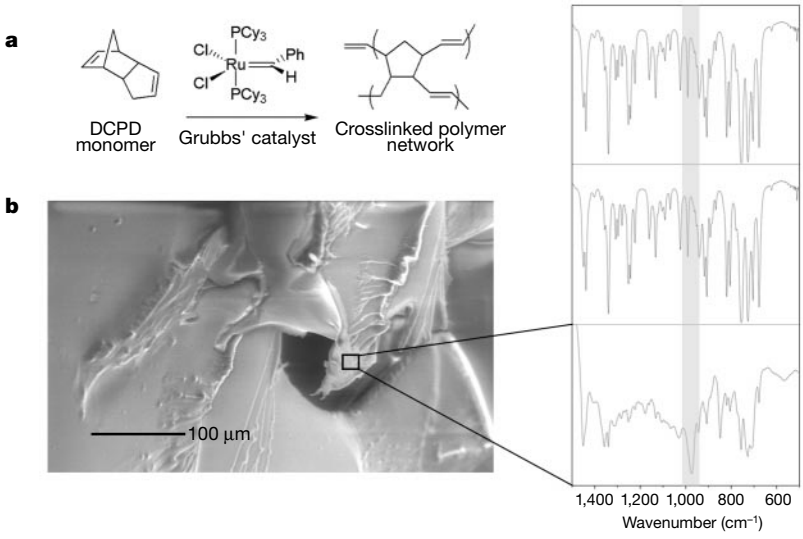

Figure 3 Chemistry of self-healing. **a**, Ruthenium-based Grubbs' catalyst initiates ring-opening metathesis polymerization (ROMP) of dicyclopentadiene (DCPD). **b**, Environmental ESEM micrograph and infrared analyses. IR spectra correspond to neat DCPD (top), an authentic sample of poly(DCPD) prepared with Grubbs' catalyst and DCPD monomer (middle), and poly(DCPD) film formed at the healed interface (bottom). The highlighted peak at 965 cm^{-1} is characteristic of *trans* double bonds of ring-opened poly(DCPD).

microscope image of the fracture plane in Fig. 2c further illustrates the rupture process of an embedded microcapsule.

Completion of the self-healing process requires a suitable chemistry to polymerize the healing agent in the fracture plane. We identified the living ring-opening metathesis polymerization (ROMP) as meeting the diverse set of requirements of the self-healing system, which includes long shelf life, low monomer viscosity and volatility, rapid polymerization at ambient conditions, and low shrinkage upon polymerization. The ROMP reaction invokes the use of a transition metal catalyst (Grubbs' catalyst) that shows high metathesis activity while being tolerant of a wide range of functional groups as well as oxygen and water[20–22]. The reaction polymerizes dicyclopentadiene (DCPD) at room temperature in several minutes to yield a tough and highly cross-linked polymer network (Fig. 3a). DCPD-filled microcapsules (50–200 μm) with a urea-formaldehyde shell were prepared using standard microencapsulation techniques. The microcapsule shell provides a protective barrier between the catalyst and DCPD to prevent polymerization during the preparation of the composite.

In order to test the stability and activity of the catalyst in an epoxy matrix, solution-state ^{1}H-NMR and solid-state ^{31}P-NMR spectroscopies of the self-healing polymer composite have been performed. Solutions of Grubbs' catalyst with the epoxy prepolymer and diethylenetriamine are chemically compatible as revealed by the characteristic benzylidene resonance at 23.3 p.p.m. Solid state ^{31}P-NMR measurements of a cured epoxy material with Grubbs' catalyst shows a characteristic signal corresponding to the tricyclohexylphosphine (PCy_3) coordinated to the ruthenium metal present in the catalyst. Solid state ^{1}H-NMR spectroscopy of the self-healing polymer composite also indicates the presence of a liquid DCPD monomer phase within the cured epoxy matrix.

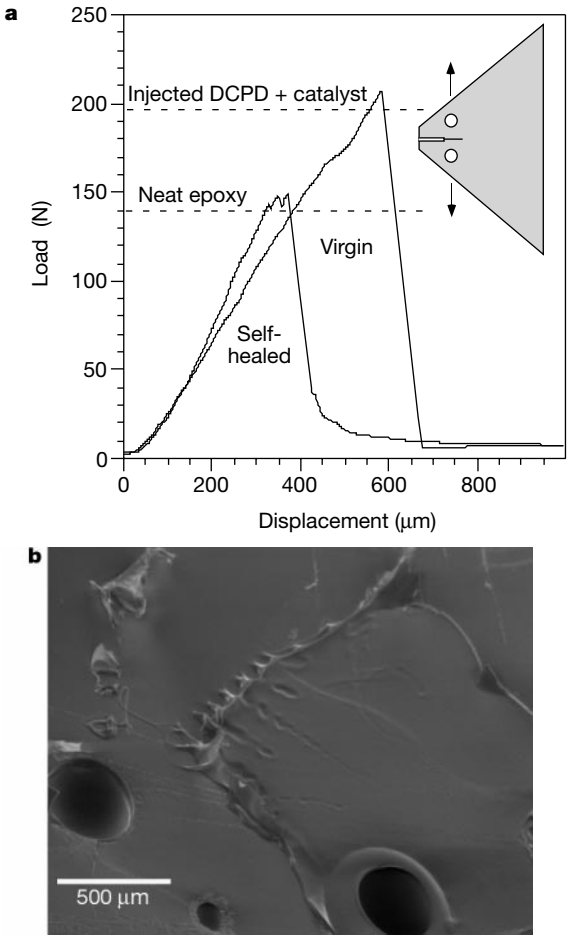

Figure 4 Self-healing efficiency in an epoxy polymer. **a**, Healing efficiency is obtained by fracture toughness testing of tapered double-cantilever beam (TDCB) specimens. The virgin fracture toughness is determined by propagating the starter crack along the mid-plane of the specimen. Subsequently, the load is removed and the crack allowed to heal at room temperature with no manual intervention. The healed fracture toughness is then measured by retesting the specimen. **b**, Post-fracture analysis of the specimens revealed that the healed crack failed in an interfacial manner from one side of the epoxy/poly(DCPD) interface to the other. The ESEM image in **b** shows one area of the fracture plane of a healed specimen in which the poly(DCPD) film is still attached to the interface on the right side of the image. The film that originally covered the interface on the left side of the image is found on the opposite mating surface of the specimen.

Evidence of polymerization of the healing agent induced by damage is provided by environmental scanning electron microscopy (ESEM) and infrared spectroscopy (Fig. 3b). ESEM micrographs reveal the presence of a thin polymer film on the fracture surface. Infrared spectroscopy of this film indicates an absorption at 965 cm^{-1} characteristic of the ring-opened product, poly(DCPD). Control samples in which the catalyst was excluded showed no ability to polymerize the DCPD monomer, providing evidence that the embedded catalyst initiated the polymerization of the healing agent.

To assess the crack-healing efficiency of these composite materials, fracture tests were performed using a tapered double-cantilever beam (TDCB) specimen (Fig. 4). Self-healing composite and control samples were fabricated. Control samples consisted of: (1) neat epoxy containing no Grubbs' catalyst or microspheres; (2) epoxy with Grubbs' catalyst but no microspheres; and (3) epoxy with microspheres but no catalyst. A sharp pre-crack was created in the tapered samples by gently tapping a razor blade into a moulded starter notch. Load was applied in a direction perpendicular to the precrack (Mode I) with pin loading grips as shown in Fig. 4a. The virgin fracture toughness was determined from the critical load to propagate the crack and fail the specimen. After failure, the load was removed and the crack allowed to heal at room temperature with no manual intervention. Fracture tests were repeated after 48 hours to quantify the amount of healing and in all of the healed samples, the crack propagated along the original (virgin) crack plane. The intrinsic ability of the healing agent to rebond epoxy is shown by the upper horizontal dotted line in Fig. 4a which represents the average fracture load achieved for control samples (1) manually healed by injecting a mixture of DCPD and Grubbs' catalyst into the crack plane.

A representative load–displacement curve for a self-healing composite sample is plotted in Fig. 4a demonstrating recovery of about 75% of the virgin fracture load. In great contrast, all three types of control samples showed no healing and were unable to carry any load upon reloading. A set of four independently prepared self-healing composite samples showed an average healing efficiency of 60%. When the healing efficiency is calculated relative to the critical load for the virgin, neat resin control (lower horizontal dotted line in Fig. 4a), a value slightly greater than 100% is achieved. The average critical load for virgin self-healing samples containing microspheres and Grubbs' catalyst was 20% larger than the average value for the neat epoxy control samples, indicating that the addition of microspheres and catalyst increases the inherent toughness of the epoxy.

Self-healing composites possess great potential for solving some of the most limiting problems of polymeric structural materials: microcracking and hidden damage. Microcracks are the precursors to structural failure and the ability to heal them will enable structures with longer lifetimes and less maintenance. Filling microcracks will also mitigate the deleterious effects of environmentally assisted degradation such as moisture swelling and stress corrosion cracking. Although the potential benefits are quite high, the specific composite described here has some practical limitations on crack-healing kinetics and the stability of the catalyst to environmental conditions.

We have thus developed a new structural polymeric material that possesses the ability to heal cracks autonomically and recover

structural function. Such materials will increase the reliability and service life of thermosetting polymers used in a wide variety of applications ranging from microelectronics to aerospace. These concepts may also be applicable to a broad class of brittle materials including ceramics and glasses. We expect that the field of self-healing, although still in its infancy, will evolve beyond the method presented here until true biomimetic healing is achieved by incorporating a circulatory system that continuously transports the necessary chemicals and building blocks of healing to the site of damage. □

Methods

Preparation of microcapsules by *in situ* polymerization

In a 600 ml beaker we dissolved urea (0.11 mol, 7.0 g) followed by resorcinol (0.5 g) and ammonium chloride (0.5 g) in water (150 ml). A 5 wt.% solution of ethylene maleic anhydride copolymer (100 ml) was added to the reaction mixture and the pH of the reaction mixture was adjusted to 3.5 using 10% NaOH solution. The reaction mixture was agitated at 454 r.p.m. and to the stirred solution we added 60 ml of dicyclopentadiene to achieve an average droplet size of 200 μm. To the agitated emulsion was added 37% formaldehyde (0.23 ml, 18.91 g) solution and then the temperature of the reaction mixture was raised to 50 °C and maintained for 2 h. After 2 h, 200 ml of water was added to the reaction mixture. After 4 h, the reaction mixture was cooled to room temperature and the microcapsules were separated. The microcapsule slurry was diluted with an additional 200 ml of water and washed with water (3 × 500 ml). The capsules were isolated by vacuum filtration, and air dried. The yield was 80%. Their average size was 220 μm.]

Self-healing epoxy specimen manufacture

The epoxy matrix composite was prepared by mixing 100 parts EPON 828 (Shell Chemicals Inc.) epoxide with 12 parts DETA (diethylenetriamine) curing agent (Shell Chemicals Inc.). Self-healing epoxy specimens were prepared by mixing 2.5% (by weight) Grubbs' catalyst and 10% (by weight) microcapsules with the resin mixture described above. The resin was then poured into silicone rubber moulds and cured for 24 h at room temperature, followed by postcuring at 40 °C for 24 h.

TDCB specimens

The TDCB sample was introduced by Mostovoy and co-workers[23] and is designed so that the compliance of the specimen changes linearly with crack length during the test. This tapered geometry enables controlled crack growth across the centre of a brittle sample such as epoxy. The fracture toughness for TDCB specimens depends only on the applied load and is independent of the crack length so that $K_{IC} = \alpha P_c$ where α is a function of geometry and material properties and P_c is the critical load at fracture. K_{IC} is the experimentally determined mode-I critical stress intensity factor. A taper angle of 40° was used and α was measured to be 7,700 $m^{-3/2}$.

Quantifying healing efficiency

Previous studies of crack healing in thermoplastic polymers quantified healing effects by comparing the fracture toughness of the virgin material to the fracture toughness measured after crack closure and healing.[13–16]. An efficiency of healing was defined as the ratio of the fracture toughness of healed and virgin materials such that $\eta = K_{IC}^{healed}/K_{IC}^{virgin}$ where η is the healing efficiency.

Received 15 August; accepted 12 December 2000.

1. Talrega, R. Damage development in composites: mechanisms and modelling. *J. Strain Anal. Eng. Des.* **24,** 215–222 (1989).
2. Talrega, R. (ed.) *Damage Mechanics of Composite Materials* 139–241 (Elsevier, New York, 1994).
3. Gamstedt, E. K. & Talrega, R. Fatigue damage mechanisms in unidirectional carbon-fibre-reinforced plastics. *J. Mater. Sci.* **34,** 2535–2546 (1999).
4. Pecht, M. G., Nguyen, L. T. & Hackim, E. B. *Plastic-Encapsulated Microelectronics* 235–301 (John Wiley & Sons, New York, 1995).
5. Lee, L. H. *Adhesive Bonding* 239–291 (Plenum, New York, 1991).
6. Wool, R. P. *Polymer Interfaces: Structure and Strength* Ch. 12 445–479 (Hanser Gardner, Cincinnati, 1995).
7. Dry, C. & Sottos, N. in *Smart Structures and Materials 1993: Smart Materials* (ed. Varadan, V. K.) Vol. 1916, 438 (SPIE Proceedings, SPIE, Bellingham, WA, 1993).
8. Dry, C. Procedures developed for self-repair of polymeric matrix composite materials. *Comp. Struct.* **35,** 263–269 (1996).
9. Wiederhorn, S. M. & Townsend, P. R. Crack healing in glass. *J. Am. Ceram. Soc.* **53,** 486–489 (1970).
10. Stavrinidis, B. & Holloway, D. G. Crack healing in glass. *Phys. Chem. Glasses* **24,** 19–25 (1983).
11. Inagaki, M., Urashima, K., Toyomasu, S., Goto, Y. & Sakai, M. Work of fracture and crack healing in glass. *J. Am. Ceram. Soc.* **68,** 704–706 (1985).
12. Jud, K. & Kausch, H. H. Load transfer through chain molecules after interpenetration at interfaces. *Polym. Bull.* **1,** 697–707 (1979).
13. Jud, K., Kausch, H. H. & Williams, J. G. Fracture mechanics studies of crack healing and welding of polymers. *J. Mater. Sci.* **16,** 204–210 (1981).
14. Kausch, H. H. & Jud, K. Molecular aspects of crack formation and healthy in glassy polymers. *Plastic Rubber Proc. Appl.* **2,** 265–268 (1982).
15. Wool, R. P. & O'Conner, K. M. A theory of crack healing in polymers. *J. Appl. Phys.* **52,** 5953–5963 (1982).
16. Wang, E. P., Lee, S. & Harmon, J. Ethanol-induced crack healing in poly(methyl methacrylate). *J. Polym. Sci. B* **32,** 1217–1227 (1994).
17. Lin, C. B., Lee, S. & Liu, K. S. Methanol-induced crack healing in poly(methyl methacrylate). *Polym. Eng. Sci.* **30,** 1399–1406 (1990).
18. Raghavan, J. & Wool, R. P. Interfaces in repair, recycling, joining and manufacturing of polymers and polymer composites. *J. Appl. Polym. Sci.* **71,** 775–785 (1999).
19. Mura, T. *Micromechanics of Defects in Solids* 2nd edn (Kluwer Academic, New York, 1987).
20. Grubbs, R. H. & Tumas, W. Polymer synthesis and organotransition metal chemistry. *Science* **243,** 907–915 (1989).
21. Schwab, P., Grubbs, R. H. & Ziller, J. W. Synthesis and applications of $RuCl_2(=CHR')(PR_3)_2$: the influence of the alkylidene moiety on metathesis activity. *J. Am. Chem. Soc.* **118,** 100–110 (1996).
22. Sanford, M. S., Henling, L. M. & Grubbs, R. H. Synthesis and reactivity of neutral and cationic ruthenium(II) tri(pyrazolyl)borate alkylidenes. *Organometallics* **17,** 5384–5389 (1998).
23. Mostovoy, S., Croseley, P. B. & Ripling, E. J. Use of crack-line-loaded specimens for measuring plane-strain fracture toughness. *J. Mater.* **2,** 661–681 (1967).

Acknowledgements

This work has been sponsored by the University of Illinois Critical Research Initiative Program and the AFOSR Aerospace and Materials Science Directorate. Electron microscopy was carried out in the Center for Microanalysis of Materials, University of Illinois, which is supported by the US Department of Energy.

Correspondence and requests for materials should be addressed to S.W. (e-mail: swhite@uiuc.edu).

A chiroselective peptide replicator

Alan Saghatelian, Yohei Yokobayashi, Kathy Soltani & M. Reza Ghadiri

Departments of Chemistry and Molecular Biology and the Skaggs Institute for Chemical Biology, The Scripps Research Institute, La Jolla, California 92037, USA

The origin of homochirality in living systems is often attributed to the generation of enantiomeric differences in a pool of chiral prebiotic molecules[1,2], but none of the possible physiochemical processes considered[1–7] can produce the significant imbalance required if homochiral biopolymers are to result from simple coupling of suitable precursor molecules. This implies a central role either for additional processes that can selectively amplify an initially minute enantiomeric difference in the starting material[1,8–12], or for a nonenzymatic process by which biopolymers undergo chiroselective molecular replication[13–16]. Given that molecular self-replication and the capacity for selection are necessary conditions for the emergence of life, chiroselective replication of biopolymers seems a particularly attractive process for explaining homochirality in nature[13–16]. Here we report that a 32-residue peptide replicator, designed according to our earlier principles[17–20], is capable of efficiently amplifying homochiral products from a racemic mixture of peptide fragments through a chiroselective autocatalytic cycle. The chiroselective amplification process discriminates between structures possessing even single stereochemical mutations within otherwise homochiral sequences. Moreover, the system exhibits a dynamic stereochemical 'editing' function; in contrast to the previously observed error correction[20], it makes use of heterochiral sequences that arise through uncatalysed background reactions to catalyse the production of the homochiral product. These results support the idea that self-replicating polypeptides could have played a key role in the origin of homochirality on Earth.

Chiroselective amplification refers to an autocatalytic process in which a homochiral template instructs the synthesis of a homochiral polymer of the same handedness[13]. Past efforts aimed at establishing the feasibility of nonenzymatic chiroselective amplification, using nucleic acids and their analogues, have been hampered by lack of template turnover[13] and/or enantiomeric cross-inhibition processes in template-directed oligomerization of activated monomeric building blocks[14–16].

The peptide used in the present study was identified using design and mechanistic principles that are similar to previously